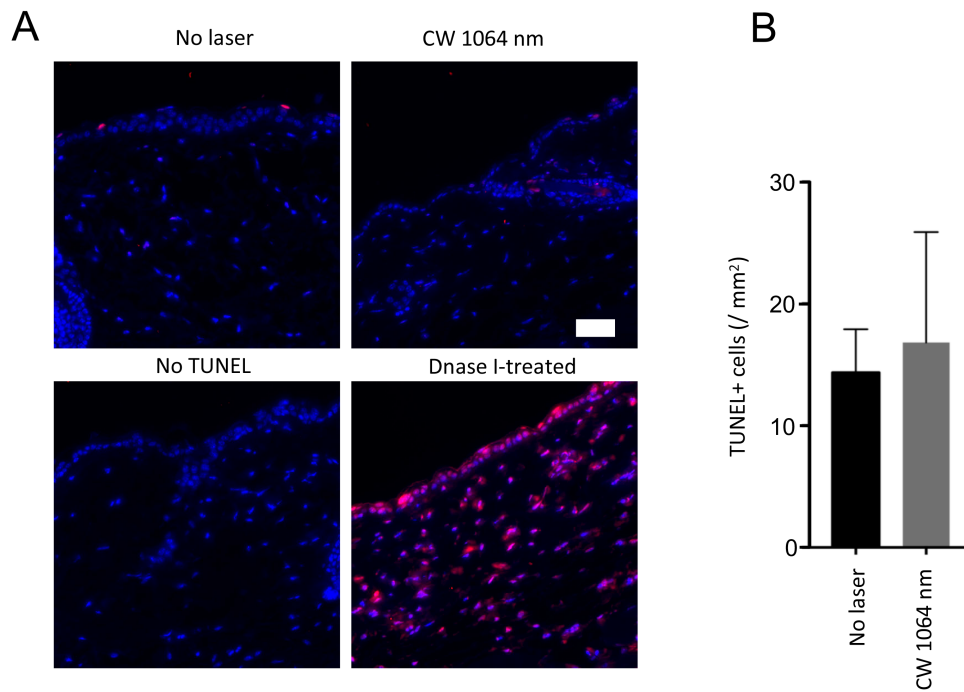


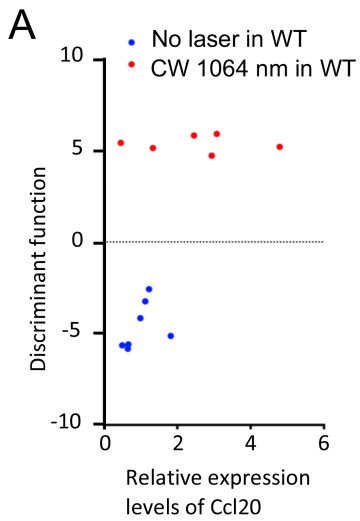
**Supplementary Figure S1. Reconstitution of sash mice with terminally differentiated cultured bone-marrow derived mast cells (BMMCs).**

**A–B**, Terminal differentiation of cultured BMMCs was examined by toluidine blue staining and flow cytometry. **A**, A representative image of cultured BMMCs stained with toluidine blue *in vitro* is shown. Bar = 50  $\mu$ m. **B**, A representative plot of BMMCs analyzed by flow cytometry is shown. Differentiated BMMCs were stained for CD117 and Fc $\epsilon$ RI. We used fully differentiated BMMCs only when 97-98 % of BMMCs were double-positive for CD117 and Fc $\epsilon$ RI $\alpha$ . **C–D**, Reconstitution of MCs with cultured BMMCs was examined by toluidine blue staining of skin biopsies. Fully differentiated  $4 \times 10^6$  BMMCs were injected into the flank skin of 4-week-old sash mice. **C**, Representative images of toluidine-stained skin tissue of the back of mice 8 weeks after the MC reconstitution. Bar = 50  $\mu$ m. **D**, Quantitation of MCs in the skin. Error bars show means  $\pm$  s.e.m.



**Supplementary Figure S2. The effect of the NIR laser on the skin tissue.**

Tissue damage in the laser-treated skin was examined by TUNEL staining. TUNEL staining was performed to detect apoptotic cells 6 hours after the CW near-infrared (NIR) laser treatment in the back skin of mice. **A**, Representative images of TUNEL-stained skin tissue are presented. Apoptotic cells were identified in red. Nuclei were identified by counter staining using DAPI. The bar indicates 50  $\mu$ m. **B**, Quantification of TUNEL<sup>+</sup> cells. Note that no significant increase in apoptotic cells was observed. Error bars show means  $\pm$  s.e.m. Representative results are shown from 2 independent experiments.  $n = 3$  for each group.

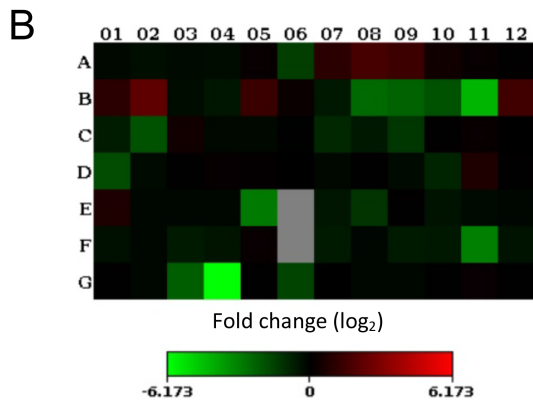
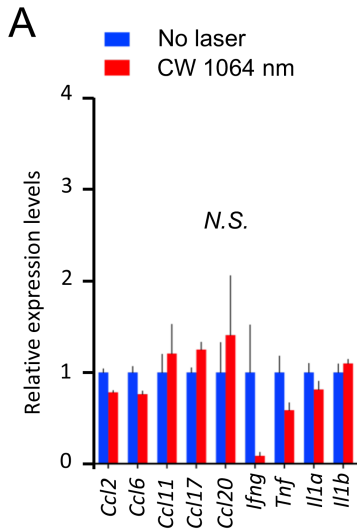


**B**

Genes	Multivariate analysis	Univariate analysis
Ccl2	30.10275055	0.29972
Ccl6	-38.34811176	0.38442
Ccl11	7.31377446	0.42976
Ccl17	1.94451778	0.41399
Ccl20	3.3547653	0.45419
Ilg	1.45979257	0.25415
Tnf	-0.70122012	-0.29116
Il1a	6.06398491	0.41102
Il1b	-5.8476513	0.23706

**Supplementary Figure S3. The effect of the NIR laser on the chemokine expression in skin.**

The effect of the NIR laser on the chemokine expression in skin in WT mice. **A**, We ran a discriminant analysis to see if the 9 selected genes of importance could predict the effect of the CW NIR 1064 nm laser treatment on the chemokine expression for the data at 6 hours in WT mice. The multivariate discriminant analysis indicated a significant discriminant function with a canonical correlation of 0.98, indicating the significant treatment effect in WT mice. A scatterplot of values for the discriminant function for each record plotted against the values of the *Ccl20* gene is shown. Note the groups overlap somewhat on the gene *Ccl20*, but are distinctly separated from each other on the discriminant function. One sample from CW 1064 nm-treated group was removed from the multivariate discriminant analysis as this sample missed Tnf expression data.  $n = 7, 6-7$  for no laser, CW 1064 nm-treated groups. Results were pooled from 3 independent experiments. **B**, Canonical coefficient in multivariate and univariate analyses for each gene. The loading coefficients for all 9 genes on the discriminant function show that Ccl2 and Ccl6 are the major determinants in the multivariate analysis where class means of the discriminant function are -4.598591451 for no laser and 5.365023360 for CW 1064 nm groups, while Cc120 is the gene most predictive (but not statistically significant) of the effect of the CW 1064 nm treatment in the univariate analysis of a point-biserial correlation of treatment groups (numeric coded -1 for no NIR and +1 for the CW 1064 nm) vs. gene expressions.



Gene	Fold changes
CCL2	1.31
CCL11	1.14
CCL17	2.7
CCL20	1.13
CCL23	2.02
IFNG	1.02
TNF	1.04
IL1A	1.03
IL1B	0.74

Layout	01	02	03	04	05	06	07	08	09	10	11	12
A	AIMP1	BMP2	C5	CCL1	CCL11	CCL13	CCL15	CCL16	CCL17	CCL2	CCL20	CCL22
B	CCL23	CCL24	CCL26	CCL3	CCL4	CCL5	CCL7	CCL8	CCR1	CCR2	CCR3	CCR4
C	CCR5	CCR6	CCR8	CD40LG	CSF1	CSF2	CSF3	CX3CL1	CX3CR1	CXCL1	CXCL10	CXCL11
D	CXCL12	CXCL13	CXCL2	CXCL3	CXCL5	CXCL6	CXCL9	CXCR1	CXCR2	FASLG	IFNA2	IFNG
E	IL10RA	IL10RB	IL13	IL15	IL16	IL17A	IL17C	IL17F	IL1A	IL1B	IL1R1	IL1RN
F	IL21	IL27	IL3	IL33	IL5	IL5RA	IL7	CXCL8	IL9	IL9R	LTA	LTB
G	MIF	NAMPT	OSM	SPP1	TNF	TNFRSF11	TNFSF10	TNFSF11	TNFSF13	TNFSF13	TNFSF4	VEGFA

**Supplementary Figure S4. The effect of the NIR laser on the chemokine expression in cultured BMDCs and keratinocytes.**

The effect of the NIR laser on the chemokine expression in fully differentiated murine BMDCs and human epidermal keratinocytes in culture. **A**, The expression of chemokines in BMDCs was measured 4 hours following the CW NIR laser treatment using qPCR. Error bars show means  $\pm$  s.e.m.  $n = 7, 7$ , for no laser control in WT, CW 1064 nm laser-treated groups, respectively. Results were pooled from 3 independent experiments. **B**, The expression of an array of inflammatory cytokines and receptors was examined 4 hours after the NIR laser treatment in keratinocytes.  $n = 4, 4$  for no laser, CW 1064 nm laser-treated groups. Representative data from two independent experiments are presented.